RESEARCH PAPER

Modeling size-density trajectories of even-aged ash (*Fraxinus excelsior* L.) stands in France. A baseline to assess the impact of *Chalara* ash dieback

Noël Le Goff[1] · François Ningre[1] · Jean-Marc Ottorini[1]

Abstract

· *Key message* **A piecewise polynomial function already used to represent the size-density trajectories of pure even-aged stands of beech, oak, and Douglas-fir proved its ability to represent the size-density trajectories of a new species, ash. The widespread ash dieback caused departures from the expected size-density trajectories. These abnormalities can be used to detect an extra level of mortality due to infection by *Hymenoscyphus fraxineus* in pure even-aged ash stands**.

· *Context* The size-density trajectories allow quantifying more precisely the density of stands and can help the forest manager to decide of the opportunity of thinnings. This study helped to quantify extra mortality in pure even-aged stands by using the size-density trajectories established for stands evolving at maximum density.

· *Aims* This study was conducted to establish size-density trajectories of pure even-aged ash stands and compare them with those recently established for beech and oak in France, in particular concerning the onset of density-dependent (regular) mortality. The additional effect of ash dieback on mortality was also an issue.

· *Material and methods* We used permanent and semi-permanent unthinned ash plots installed in the north of France and where inventories of trees were performed at more or less regular intervals: measurements included tree status (dead or alive) and diameter or girth at breast height for all trees and total height for a sample of living trees. The size-density trajectories of plots describing the course of the number of living trees in relation with the mean stand girth, in logarithmic scales, were modeled with a piecewise polynomial function fitted with a mixed-effects model. A permanent sample of trees was also selected for ash dieback and extra mortality monitoring.

· *Results* The piecewise polynomial function already used proved its ability to represent the size-density trajectories of even-aged ash stands of various initial densities and fertility levels. As for beech and oak, the trajectories were modeled so that mortality onset occurred at a constant relative density. This level appeared to be much higher for ash (RDI = 0.58), revealing that ash survived with less growing space than beech and oak and appeared to be more efficient. Ash dieback caused an additional mortality in the experimental ash stands studied, and this excess of mortality appeared predictable on the basis of observed departures from the expected size-density trajectories.

· *Conclusion* A single parameter function family could be used to predict the size-density trajectories of even-aged ash stands, on the basis of the results obtained previously on oak and beech. Mortality onset and space requirements of ash could be compared with those of beech and oak and show that ash can survive at higher densities and is a more efficient species. Predicted size-density trajectories proved also useful to detect and quantify the excess of mortality due to *H. fraxineus* on ash. This approach could be extended to other diseases and species with predictable size-density trajectories.

Handling Editor: John M Lhotka

This article is part of the Topical Collection on *Mensuration and modelling for forestry in a changing environment*

✉ François Ningre
   francois.ningre@inrae.fr

[1] Université de Lorraine, AgroParisTech, INRAE, UMR Silva, 54000 Nancy, France

1 Introduction

The work reported here is a natural continuation of previous studies aimed at modelizing the size-density trajectories of pure even-aged stands. Thus, it follows the studies already conducted on beech (*Fagus silvatica* L), Douglas fir

(*Pseudotsuga menziesii*), and oak (*Quercus petraea* (Matt.) Liebl.) (Ningre et al. 2016a, 2016b, 2019). Size-density trajectories aim at predicting natural mortality—only due to intra-specific competition—in stands maintained at maximum density (no thinning treatment) and thus relate the number of trees per hectare in stands (*N*) to their mean girth at breast height (*Cg*) in logarithmic scales.

In the near past, a maximum linear size-density relationship could be obtained for pure even-aged ash stands in France (Le Goff et al. 2011), which constituted the last part of the trajectories for stands of various initial densities. More recently, a model was built for beech and oak which represented the whole size-density trajectory: stands stay at initial density until mortality appears (mortality onset), then decrease gradually in density until reaching the maximum size-density line, and then continue to decrease in density while following this line. As raised by Ningre et al. (2019), useful discussions of self-thinning of forest stands, and maximum size-density can be found in Johnson et al. (2009) and in Lhotka and Loewenstein (2008), with references on past works on the subject.

As the appropriate data for modelizing the ash size-density trajectories were scarce, the hypotheses used to obtain those trajectories were based on features already observed with beech, oak, and Douglas fir (Ningre et al. 2016a, 2016b, 2019). The ash data came principally from permanent plots established in the north and northeast of France during the 1980s to study the effects of different thinning treatments on growth and development of pure even-aged ash stands. Unfortunately, during the last years—that is, approximately since year 2012—ash stands in the north and northeast of France were subject to infection by *Hymenoscyphus fraxineus*[1] (Goudet and Piou 2012) causing dieback and mortality of trees. Thus, the last growth period (after year 2012) was not considered for fitting the size-density trajectories of ash. However, data after 2012 were used to analyze the effects of ash dieback on stand characteristics by comparing the observed size-density trajectory to the expected trajectory of a healthy ash stand (without *Chalara*) of the same initial density. The expected size-density trajectory could then be used in the same way as the baseline defined by Manion and Griffin (2001) to characterize the excess of mortality in mixed uneven aged forests in the USA.

The objectives of the study were then:

– to evaluate the ability of the size-density trajectory model established for other species to represent the size-density trajectories of pure even-aged stands of ash with variable initial densities and growing on sites of different fertility

– to evaluate the potential of the modelized size-density trajectories to detect the first signs of ash dieback in even-aged ash stands on the basis of stand characteristics (number of live trees for a given mean stand girth)

2 Materials and methods

2.1 Ash plots

The ash data came essentially from two networks of permanent and semi-permanent plots installed in the north and the northeast of France (Annex, Fig. 8).

The first set of permanent plots (set #1, Table 1) belongs to a network installed in the 1980s period to study the effects of thinnings on the dynamics (growth and mortality) of pure even-aged ash stands. For the present study, only the unthinned plots of this network ("control plots") were considered. The stands originated from natural regeneration or from plantation establishment and covered a wide range of densities at the origin (from 1100 to 40,000 trees ha^{-1}). An old additional plot, Fleur-Fontaine, installed in 1907, was also considered but only for the period before thinning.

The second set of semi-permanent plots (set #2, Table 1) was installed later to study more specifically the dynamics of stands at maximum density. These plots are generally young stands originating from natural regeneration, and only those where regular mortality had not started at installation were retained for the study, with the exception of the plot of Amelécourt which could however be related to the treatment "80,000" considering its initial density (Table 1). The 4 semi-permanent plots retained for the study (Amelécourt-3, Arracourt-8, Vic-sur-Seille-10, Vic-sur-Seille-11) represented the highest densities observed in the whole data set. More details on these plots can be found in a preceding study (Le Goff et al. 2011).

For the set #1 plots, in some cases, the initial density differed greatly from the original density: this was the case for the plots of Aibes, Hardelot, and Val-St-Pierre. This is due to cleaning operations performed at the installation of those plots, so as to lower the initial stand density and at the same time reduce the importance of species mixed with ash as natural regeneration (Val-St-Pierre). It was then hypothesized that the density trajectories after such cleaning operations followed the same pattern as that of stands of the same corresponding initial density, as it was already observed for beech (Ningre et al. 2016a).

Ash dieback was detected in our experimental stands as soon as year 2012, in accordance with the observations made by the *French Forest Health Survey* system in the north of France (Goudet and Piou 2012). In a part of set #1 permanent plots, a survey of ash dieback was performed relying on a

---

[1] The first signs of ash dieback due to *H. fraxineus* in France were recorded in the east of France (HauteSaône) as soon as 2007 (Grandjean and Macaire 2009).

Table 1 The network of unthinned permanent (set #1) and semi-permanent (set #2) plots used to analyze the size-density trajectories of ash stands originating either from plantations (P) or natural regenerations (R)

Data set	P or R density	Origin	Plot area	Treatment	Locality/Department	Plot	Age range	Initial density (trees ha^{-1})	
#	(trees ha^{-1})		(m^2)			#		Plot	Mean
1	1100	P	2101	900	Hérissart / 80	11	10–30	914	927
	1100	P	2074		Hérissart / 80	21	10–30	940	
	2000	P	1279	1100	Aibes / 59	1	14–34	1118	1109
	2600	P	2000		Hardelot / 59	3	15–34	1100	
	1600	P	308	1200	Brouennes / 55	4	31–43	1169	1169
	1600	P	284	1600	Brouennes / 55	5	31–44	1549	1572
	^{a}-	R	1900		Fleur-Fontaine / 54	1	12–34	1595	
	40,000	R	1763	7000	Val-St-Pierre / 02	1	10–27	7158	7158
	40,000	R	1538	8000	Val-St-Pierre / 02	4	10–27	8225	8225
2	–	R	50	80,000	Amelécourt / 57	3	18–23	49,139	82,494
		R	28		Arracourt / 54	8	13–18	88,773	
		R	28		Vic-sur-Seille / 57	11	7–12	104,704	
		R	28		Vic-sur-Seille / 57	10	7–11	87,358	

^{a} Unknown

permanent sample of about 50 trees representing the range of stand diameters in each plot.

In this study, size-density trajectories were modelized for the period prior to mortality due to *H. fraxineus*, that is, until year 2012. These modelized trajectories will constitute a baseline to characterize the excess of mortality starting in 2013.

2.2 Ash measurements

Girth (or diameter for small trees)[2] at breast height was measured yearly in each plot on all alive trees (except for the oldest plot—Fleur-Fontaine—where measurement intervals were longer). This allowed the calculation of the density (N, number of trees per ha), basal area (G, m^2 ha^{-1}), and mean girth (Cg, cm) of living trees for all plots by inventory year. The number of inventory years varied, respectively, from 11 to 21 for permanent plots and from 6 to 8 for semi-permanent ones.

Total height was also measured for a representative sample of trees in each plot at more or less regular year intervals (from 1 to 6-year intervals) during the observation periods (Annex, Fig. 8), except for the plot Fleur-Fontaine with no height measurements. This allowed the calculation of the dominant height (Ho)[3] of plots for each year presenting height samples, using the second-order polynomial height-girth curve

calculated for the appropriate year. The dominant height-age curves obtained revealed that ash plots were established on sites of variable productivity, Ho at 25 years old (Ho_25) varying from about 13 to 21 m for plots of set #1, which corresponds to medium to good sites for ash (Pilard-Landeau and Le Goff 1996). However, size-density trajectories are known to be, to a large extent, independent of site quality (Long et al. 2004; Long and Vacchiano 2014), as it was already noticed for the last part of the trajectory (maximum size-density line) as early as 1933 by Reineke. Nevertheless, size-density trajectories remain site-dependent in terms of their rate of change, which will be higher as the site quality is better.

Infection by the *H. fraxineus* is observed in six permanent plots of our research network on ash (set #1; Table 1), each year from 2012 to 2015 and in 2018. Ash dieback was followed in each plot on the permanent sample of trees selected in 2012 by estimating the percentage of defoliation in the tree crown in summer after a careful examination of the status (alive or dead) of branches and shoots in the crown (Annex, Fig. 9). Tree health status was determined by using a protocol adapted from "DEPERIS" (Goudet et al. 2018) which allowed the characterization of tree dieback on a scale of 0 to 5, depending on shoot mortality level[4]: 0 for no shoot mortality, 1 for 1 to 10% of shoot mortality, 2 for 10 to 50% of shoot mortality, 3 for

---

[2] For trees below 3-cm diameter, the measurement of girth is difficult if not impossible.
[3] Ho was defined as the mean height of the 100 largest trees per hectare for each plot at the time of measurement.

[4] Dieback notation does not include natural pruning or mortality of shoots aged 3 years or more.

50 to 75% of shoot mortality, 4 for 75 to 99% of shoot mortality, and 5 for dead trees.

2.3 Size-density curve modeling and statistical analysis

The ash plots were grouped into 7 classes of comparable initial stand density, named "treatments" (see Ningre et al. 2019), resulting in the following initial density treatments: 900, 1100, 1200, 1600, 7000, 8000, and 80,000 trees ha^{-1} (Table 1).

The size-density modeling framework developed for beech (Ningre et al. 2016a) and oak (Ningre et al. 2019) was applied in this paper to represent the size-density trajectories of ash. The ash data (Ningre 2020) were somehow incomplete for semi-permanent plots (set #2) being followed over a relatively short period (5 to 6 years), which did not allow fitting independently the size-density trajectories, as was done for the previous studies to perform statistical tests. But, we thought that we could recover information lacking for each individual stand with a global fit at "treatment" level that is fitting at the same time the size-density trajectories of each group of plots defined by its density treatment. Moreover, we used the hypothesis[5] of inflection points marking mortality onset occurring at a constant relative density, which was previously observed (Ningre et al. 2019).

As for beech and oak, the evolution of the number of trees per hectare (N), from the early sapling stage to any stage after maximum RDI has been reached, is modeled by the following family of continuous smoothed functions f of Cg, depending only on the four parameters Cg_0, N_0, a, and b:

$$Ln(N) = f(Cg_0, N_0, a, b, Cg) \qquad (1)$$

$$= \begin{cases} & Ln(N_0) & if\ 0 < Cg \le Cg_0 \\ p+ & qLn(Cg) \quad +r\,(Ln(Cg))^2 & if\ Cg_0 < Cg \le Cg_1 \\ a+ & bLn(Cg) & if\ Cg > Cg_1 \end{cases}$$

where:

- Cg is the mean girth at breast height of the stand with N trees per hectare
- Cg_0 is the mean girth at breast height of the stand at the onset of regular mortality and N_0 its number of stems per hectare prior to this onset
- Cg_1 is the stand mean girth at breast height when the maximum RDI is reached. Cg_1 is fully determined by Cg_0 and N_0 as follows:

$$Ln(Cg_1) = \frac{2(Ln(N_0)-a)-bLn(Cg_0)}{b} \qquad (2)$$

- a and b are the parameters of the maximum size-density line:

$$Ln(N) = a + bLn(Cg) \qquad (3)$$

The size-density trajectory defined by Eq. (1) is therefore represented, in loglog scales, as the sequence of a straight line (Cg between 0 and Cg_0), a second-order polynomial with coefficients p, q, and r (Cg between Cg_0 and Cg_1) and another straight line—the maximum size-density line—(Cg over Cg_1).

Equation (1) only depends on the parameters Cg_0, N_0, a, and b (for more details see Annex, Fig. 10). The continuity constraints on this equation and its derivative imply the following relationships:

$$\begin{cases} p = & Ln(N_0) & +\dfrac{bLn(Cg_0)^2}{4Ln(\mathrm{RDI_0})} \\[2mm] q = & -\dfrac{b^2 Ln(Cg_0)}{2Ln(\mathrm{RDI_0})} \\[2mm] r = & \dfrac{b^2}{4Ln(\mathrm{RDI_0})} \end{cases} \qquad (4)$$

where RDI_0, the density at mortality onset, is equal to $\frac{N_0}{e^a Cg_0^b}$

We could satisfactorily fit Eq. (1) globally to the ash data with the constraint of the inflection points of the trajectories aligned parallel to the maximum size density line, as it was the case for beech and oak (Ningre et al. 2019). Equation (1) was fitted to the ash data using a mixed-effects model (Annex, Fig. 10), where b was a fixed parameter common to all treatments, and, as graphical analysis suggested it, a had a mean value common to all treatments with an added normal random effect due to variability from stand to stand. N_0 was a fixed parameter for each treatment. An additional parameter a_1, common to all treatments, was used to formulate the hypothesis of the inflection points being located on a line parallel to the maximum size-density line:

$$Ln(N_0) = a_1 + bLn(Cg_0).$$

The respective parameters of the fits of Eq. (1) for ash, beech, and oak were compared as well as the characteristic points of the size-density trajectories (mortality onset and reach of maximum size-density line).

Finally, the effects of ash dieback on the dynamics of stands were also examined through the size-density trajectories modifications observed after the first signs of ash dieback (twigs mortality coupled with foliage reduction) followed by mortality of the infested trees.

---

[5] Without this hypothesis, the fit could not be carried out.

Fig. 1 Size-density trajectories obtained by fitting Eq. (1) to the data of the ash plots grouped by density treatment, with alignment of the inflection points parallel to the maximum size-density line
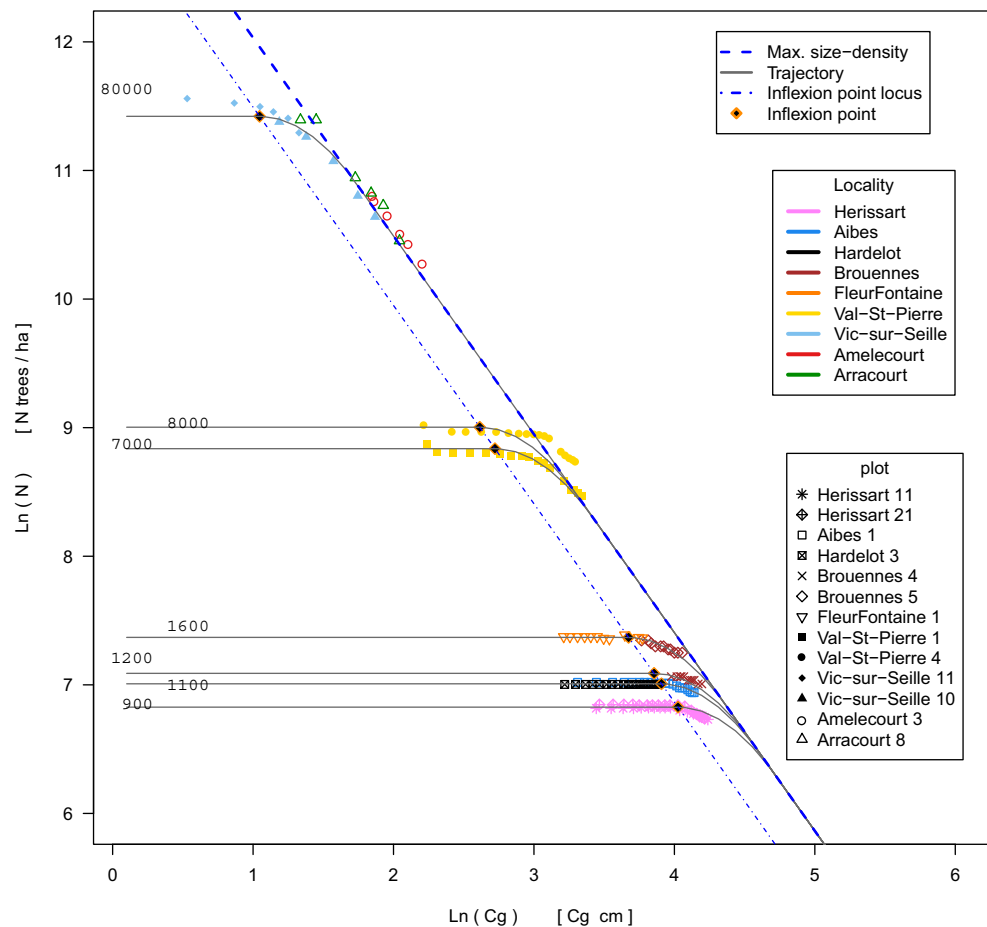
3 Results

3.1 Size-density trajectories of unthinned stands

Equation (1) was fitted to the ash data, with the constraint of alignment of the inflection points parallel to the maximum size-density line. We assumed also that there was a random effect due to plots for the parameter a. Moreover, the year to year correlations of the within group residual errors were taken into account (correlation structure "ARMA" in R, nlme), as well as the variability of these residual error dispersions across the plots (heteroscedasticity), which conducted to consider two relatively homogeneous groups of plots[6] when fitting the data (Annex, Fig. 10).

Resulting from this fit, Fig. 1 shows the fitted trajectories for each treatment with the inflection points aligned parallel to the maximum size-density line, together with the observed plot data. The normalized—corrected to allow for plot discrepancies and autocorrelation—residuals of the fit relative to the fitted values did not show time dependence, which is consistent with the graphics presentation of their empirical

autocorrelation function (Annex, Fig. 11). The residuals appeared unbiased and did not show a marked heteroscedasticity (Fig. 2). The within-group (treatment) errors appeared also normally distributed (Annex, Fig. 12). Finally, the normality of the random effect for the parameter a is also assessed by a QQ plot (Annex, Fig. 13).

The fitted size-density trajectories of each plot (Fig. 3), obtained by taking account of the random effect for the parameter a, show the reduction of the dispersion of the residuals of the fit obtained in this case, allowing to reduce the bias and uncertainties on the fixed parameters.

Table 2 gives the parameters and statistics of the fit of Eq. (1) with the constraints of alignment of the inflection points parallel to the maximum size-density line. Relying on this fit, we derived stand characteristics for the various treatments at the critical stand development stages corresponding to the onsets of mortality and reaches of maximum RDI, respectively, (N_0, Cg_0, RDI_0) and (Cg_1, N_1) (Table 3).
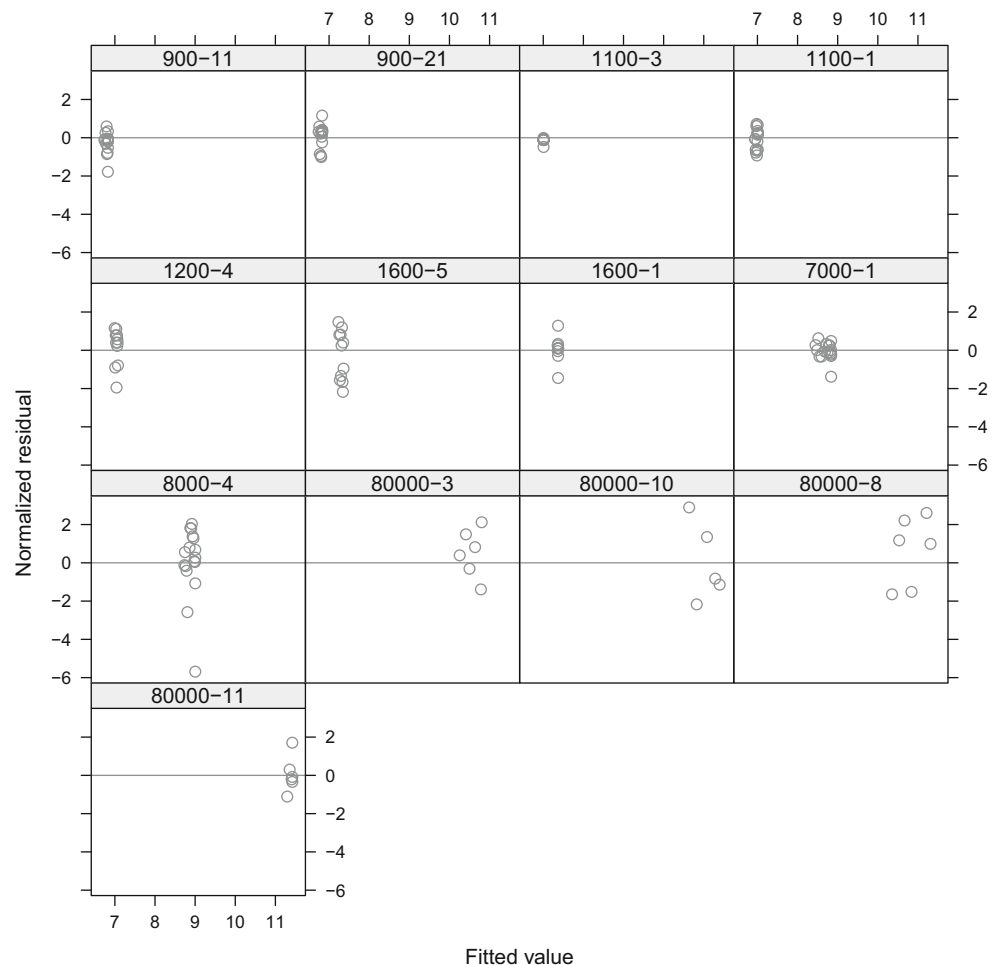
3.2 Size-density trajectories of the stands affected by ash dieback

Figure 7 presents the observed size-density trajectories of the ash plots considered in this study and affected lately by ash

---

[6] Group 1: 900–11; 900–21; 1100–3; 1100–1; 1200–4; 1600–5; 1600–1; 80,000–3; 8000–4; 80,000–10. Group 2: 7000–1; 80,000–11; 80,000–8 (plots identified by "treatment" followed by plot number)

Fig. 2 Normalized residuals for each group of ash plots in relation to the size-density trajectories values obtained by fitting Eq. 1 with alignment of the inflection points parallel to the maximum size-density line. Each panel is identified with the format "treatment-plot"

dieback, together with the predicted trajectories obtained from Eq. (1) including the random effect for the parameter a due to plot-to-plot variations. The effect of ash dieback on the size-density trajectory of each affected plot appears clearly through the lower level of density (number of alive trees per ha) for the observed Cg values. Conditional 95% confidence intervals for the fitted size-density trajectories were based on the mean 95% confidence intervals[7] of the two groups of plots with homogeneous residuals (cf. & 3.1). Also indicated on this figure are the points of the onset of maximum density for the trajectory fitted for each plot, as well as the relative density of plots in 2012, the year of the first signs of ash dieback.

3.3 *Chalara* ash dieback dynamics

The permanent sample of trees selected in each plot retained to follow the dynamics of ash dieback, allowed characterizing the evolution of mortality at individual and population levels in each selected plot. The distribution by girth at breast height in 2013 of alive and dead trees in 2018 is presented in Fig. 4 for the different

plots of variable initial density: it shows that, on average, trees that died were smaller in 2013 than trees that survived. Cumulated mortality (in %) due to ash dieback increased more or less rapidly since 2013, the year of mortality onset, until 2018 (Fig. 5). The highest levels were reached in Hardelot, Aibes, and Val-St-Pierre (between 60 and 80% of cumulated mortality).

4 Discussion

4.1 Size-density trajectory model

The piecewise size-density trajectory model already fitted for several species in France (oak, beech, and Douglas-fir) proved again adequate to represent the size-density trajectories of ash stands of different initial densities. In particular, the main hypothesis of alignment of the inflection points parallel to the maximum size-density line proved adequate to fit the observed trajectories. Moreover, differences in site quality among the ash stands sampled and the cleaning operations performed early in stand development for some plots did not seem to affect the model's ability to appropriately characterize size-density relationships present in our field data.

---

[7] These confidence intervals are not the usual confidence intervals of prediction, but rather the confidence intervals given the fitted trajectories.

Fig. 3 Observed and predicted size-density trajectories of the ash stands obtained with the fit of the model defined by Eq. (1) and the constraint of alignment of the inflection points parallel to the maximum size-density line. The plain line is the prediction at the plot level including the random effects due to stand-to-stand variations. The figure does not show any lack of fit
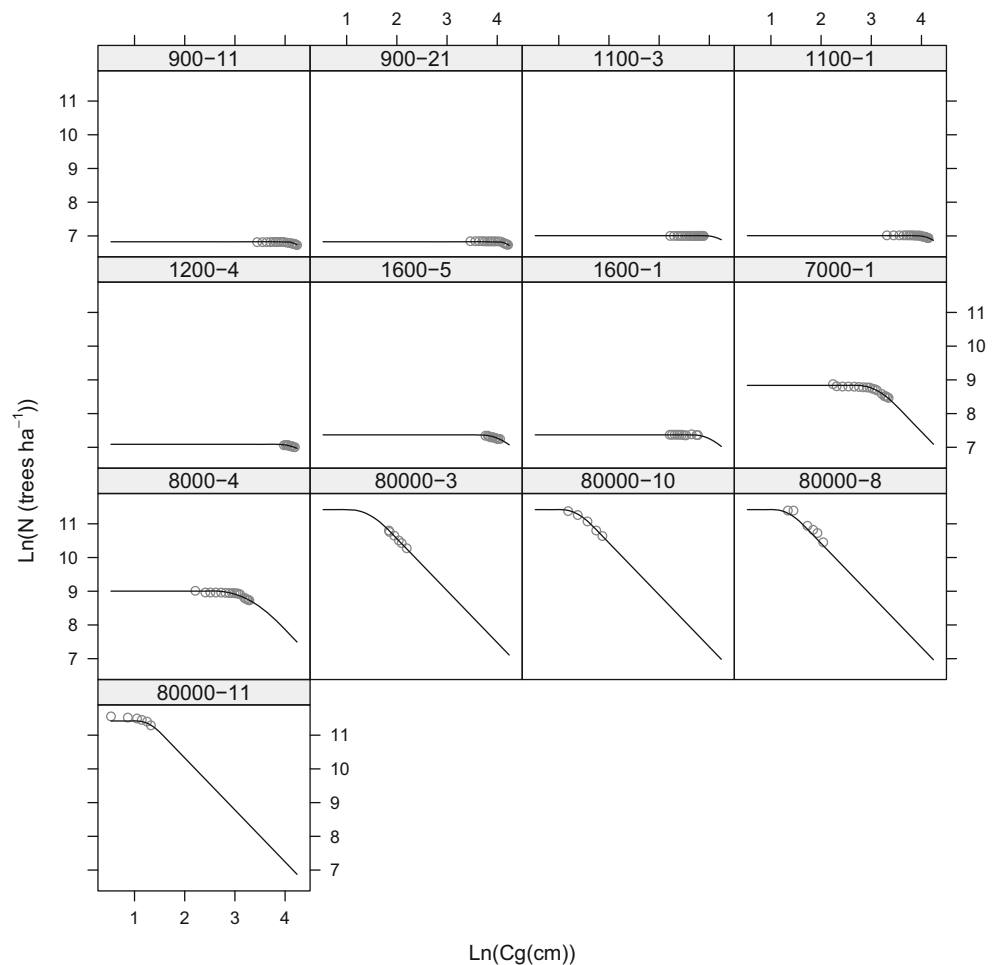
Table 2 Parameter estimates and statistics of Eq. (1) fit to the ash experimental stand data with the constraints of alignment of the inflection points parallel to the maximum size-density line

Parameter	Treatment	Observed value[†]	Estimate	Std. error	t value	P value
a	all	–	13.57	0.106	128.1	< 0.01[‡]
b	all	–	−1.54	0.019	−81.6	< 0.01
a_1	all	–	13.03	0.061	213.4	< 0.01
N_0 (trees ha^{-1})	900	927	922[¶]	7.524	122.5	< 0.01
	1100	1109	1106	8.307	133.1	< 0.01
	1200	1169	1199	23.486	51.1	< 0.01
	1600	1572	1586	14.246	111.3	< 0.01
	7000	7158	6881	459.827	15.0	< 0.01
	8000	8225	8131	118.086	68.9	< 0.01
	80000	82494	91215	1867.844	48.8	< 0.01
Residual std. deviation = 0.0167; df = 145						

[†] Mean of observed values in a treatment

[‡] Far smaller than the 0.01 standard probability level

[¶] Rounded to the nearest integer

The mixed-effects model fitted to the size-density trajectories of ash required only a random effect for the parameter a of the model to take account of variations among ash plots. This random effect appeared to some extent correlated to the site index (Ho_25) of permanent plots ($R^2 = 0.21$), but this would need to be confirmed.[8] The other parameter of the maximum

size-density line, b, was fit as a fixed parameter. The fixed values of a (13.57) and b (−1.54) are close to those obtained previously with a larger data set, but restricted to plots close to the maximum size-density line, respectively, 13.69 and −1.57 for a and b (Le Goff et al. 2011).

The size-density trajectory model fit adequately the ash data, although these data were incomplete. Then, it would have been desirable to confirm these results with additional

---

[8] Ge et al. (2017) found that, for China fir, the slope parameter b of the self-thinning line was dependent on site quality.

Table 3 Stand characteristics estimated by Eq. (1) with the added constraint of alignment of the inflection points parallel to the maximum size-density line, when fitted to the ash data

Treatment	Initial density	Estimated initial density (N_0) (trees ha^{-1})	Cg_0 (cm)	RDI_0	Cg_1 (cm)	Density at max. RDI (N_1) (trees ha^{-1})
900	927	922	56.0		112.8	537
1100	1109	1106	49.8		100.3	644
1200	1169	1199	47.2		95.2	699
1600	1572	1586	39.4	0.58	79.4	924
7000	7158	6881	15.2		30.6	4010
8000	8225	8131	13.7		27.5	4739
80000	82494	91215	2.8		5.7	53157

Fig. 4 Distribution of tree girths at breast height at mortality onset due to *Hymenoscyphus fraxineus* (2013), for alive and dead trees until 2018 in the plots monitored for ash dieback
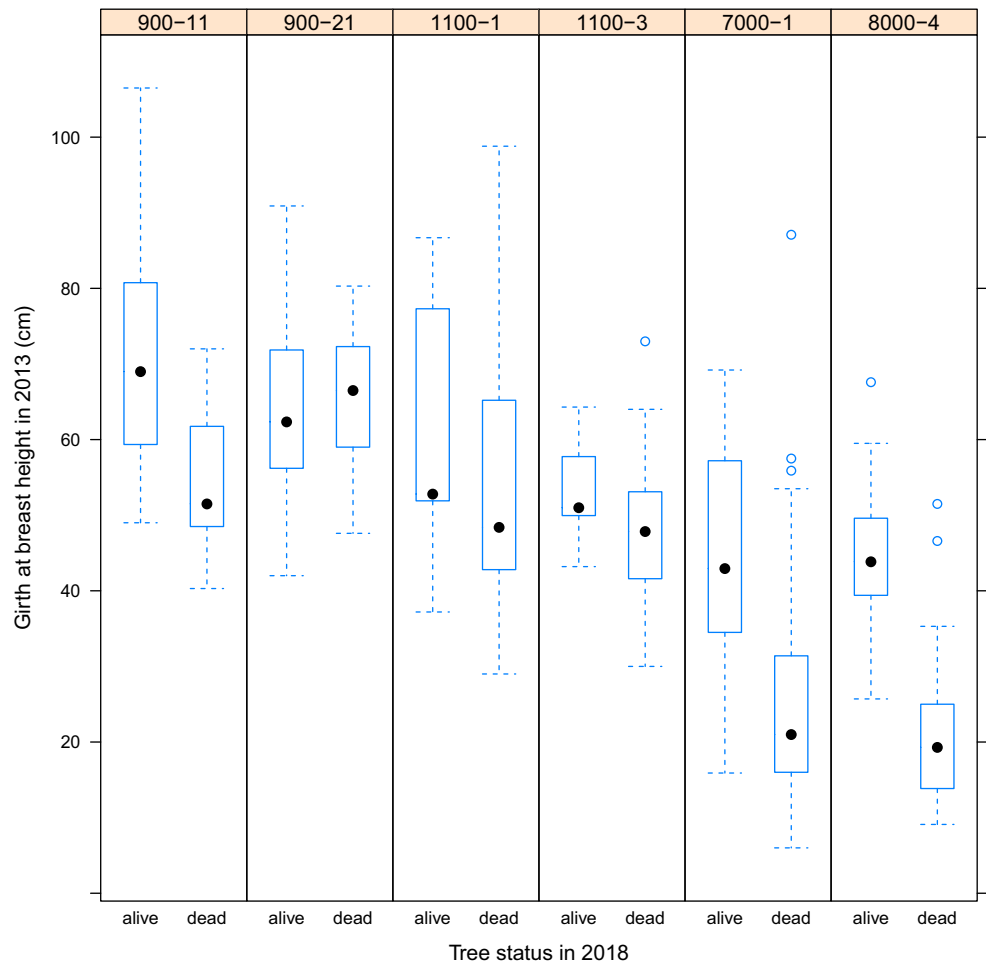
data. Unfortunately, *H. fraxineus* has spread very quickly in France, and mortality has affected greatly our network of permanent plots.

The conditional confidence intervals of the fitted size-density trajectories are rather empirical, but they allow one to postulate if an unthinned stand of ash is affected by ash dieback: this happens when the representation of the stand in (Log(N), Log(Cg)) scales falls below the theoretical size-density trajectory of the stand[9] and outside its confidence intervals.

---

[9] Theoretically, the size-density trajectory of a stand of known initial density depends on the stand for the value of the parameter *a* due to a random effect, but this effect is relatively low (comprised between 0 and 3% of the fixed value).
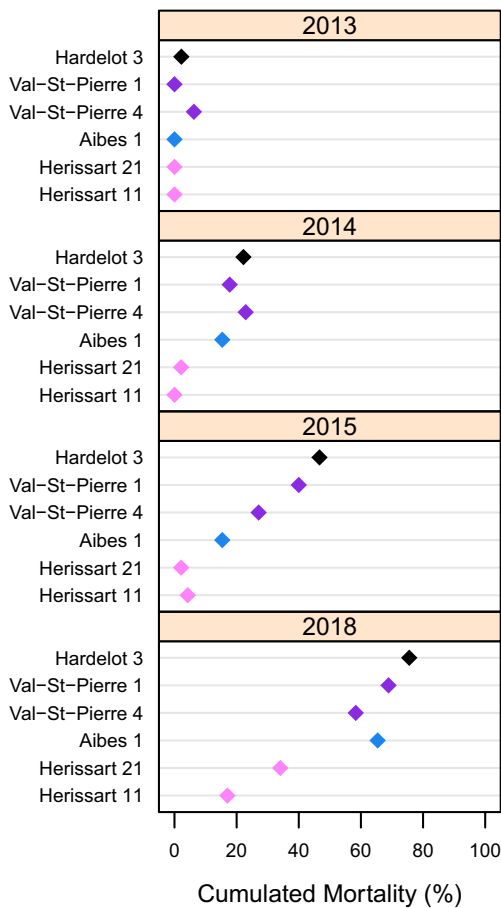
Fig. 5 Cumulated mortality (in %) due to ash dieback from 2013, the year of mortality onset, until 2018 for the permanent sample of trees of the ash plots of set #1 still followed during this period

4.2 Size-density trajectories of ash compared to those of beech and oak

The parameters of the maximum size-density line of ash (a and b) are very close to those of beech, as already seen (Le Goff et al. 2011). The parameter b appears somehow higher for oak, reflecting a steeper slope of the maximum size-density line of oak compared with that of ash and beech, while the parameter a is not significatively different for the three species (Table 4).

While ash and beech present a comparable maximum size-density line, the onset of mortality happens at a relatively higher density RDI_0 for ash than for beech or oak (0.58 compared with 0.29 and 0.35, respectively). Then, ash can better support overcrowding than beech and oak.

The size-density lines at mortality onset ($\mathrm{Ln}(N) = a_1 + b\ \mathrm{Ln}(Cg)$) and at maximum density ($\mathrm{Ln}(N) = a + b\ \mathrm{Ln}(Cg)$) can be expressed in terms of average growing space per tree ($1/N$) (Ningre et al. 2019). Figure 6 presents the variations of the average growing space per tree (s) with mean stand diameter (Dg) at mortality onset (s_0) and at maximum density (s_m) for ash, oak, and beech. It appears that, for a given Dg, the average growing space at mortality onset was much lower for ash than for beech and, a fortiori, for oak, which meant that more trees could stay alive in the case of ash and that ash was more efficient than beech and oak in its space requirements at this development stage. This is in line with the observations of Van Miegroet (1956) who found that ash can survive at high densities, the suppressed trees staying alive for a long time. However, at maximum density, it appears that the average growing space is a little higher for ash than that it is for beech: both species appear more efficient than oak for space requirement at this development stage, but ash appears to be a little less efficient than beech.

4.3 Mortality control of ash

Working with unthinned oak stands (Ningre et al. 2019), we established a relationship between the cumulated mortality and the relative stand density (RDI), which could help to control mortality. Namely, the stands with a given relative number of surviving trees (N_t/N_0), where N_t is the number of trees per hectare observed at some time t, have a constant RDI value, and the locus of the points corresponding to a given mortality rate for the trajectories of various initial stand densities is a line parallel to the maximum size-density line. For ash, which follows the same size-density model as oak (with different parameters values), we have the same property. If we consider the level of 10% cumulative mortality as a limit to perform the first thinning, this means that it is possible to wait

Table 4 Estimated parameters (a, b, $a1$) of the size-density trajectories (with their confidence intervals) and relative density at mortality onset ($RDI0$) for ash (this paper), beech, and oak (Ningre et al. 2019)

Species	Size density trajectories parameters									RDI$_0$
	a			b			a_1			
	Lower	Est.	Upper	Lower	Est.	Upper	Lower	Est.	Upper	
Ash	13.37	13.57	13.78	−1.58	−1.54	−1.51	12.92	13.03	13.15	0.58
Beech	13.30	13.58	13.86	−1.58	−1.51	−1.45	12.09	12.33	12.58	0.29
Oak	13.56	13.73	13.91	−1.69	−1.65	−1.61	12.26	12.69	13.13	0.35

Fig. 6 Comparison of the average growing space of trees (s, m^2/tree) at mortality onset and at maximum density for ash, beech and oak

with ash until *RDI* reaches the value of 0.85, whereas it is necessary to operate "earlier" with oak and beech, respectively, when the *RDI* reaches 0.62 and 0.53. This can help the forest manager to better control the density of ash in pure even-aged stands (unfortunately becoming rare) or possibly in mixed even-aged stands (where ash would appear in patches) in order to limit natural mortality of trees.

4.4 Effects of ash dieback on size-density trajectories

Ash dieback appeared lately in our ash network and of course our observations did not meet the requests of a planned experiment. In particular, the age at which the dieback began was relatively similar for all plots (dieback was not monitored in the youngest plots of our network), and we lacked replication within some density classes. However, the different patterns of size-density trajectories observed among the experimental plots, in connection with ash dieback, proved very informative even if they do not allow for size-density models to be parameterized for ash stands subjected to dieback.

The size-density trajectories of stands, after the first signs of ash dieback, depart from the expected size-density trajectories (Fig. 7). This is due to two factors:

the decrease of diameter growth of infected trees (ongoing study) and the mortality of the trees more severely infested and nearly completely "defoliated." It appeared that ash dieback was more or less pronounced depending on the site: dieback appeared the most important in Hardelot (1100–3), Val-St-Pierre (8000–4), and Aibes (1100–1). In those sites, the departure from the expected size-density trajectories—as soon as (*Cg*, *N*) falls outside of the confidence interval—happened earlier (2014 or 2015), that is, 2 or 3 years after the appearance of the first signs of infection by *H. fraxineus*. It took more time in the site of Hérissart (900–11 and 900–21) to observe such a departure (6 years) reflecting probably a less pronounced infection in that site (Fig. 7). This is in accordance with the mortality levels observed on the permanent tree sample in the different sites from the beginning of the infection (Fig. 5). The observed discrepancies between sites may be in relation with the east-west disease progression in France. However, planted (Hardelot, Aibes) or naturally regenerated stands (Val-St-Pierre) appeared equally affected by ash dieback.

Ash trees may partially recover after infection by *H. fraxineus*, for example, by producing new shoots on the stem and branches in reaction to shoots mortality. But this is

Fig. 7 Observed size-density trajectories of the ash stands extended to years following the first signs of infection by *Hymenoscyphus fraxineus* (2012), together with the predicted size-density trajectories (as observed in Fig. 3). 95% confidence intervals around the fitted curves are also represented (see text)
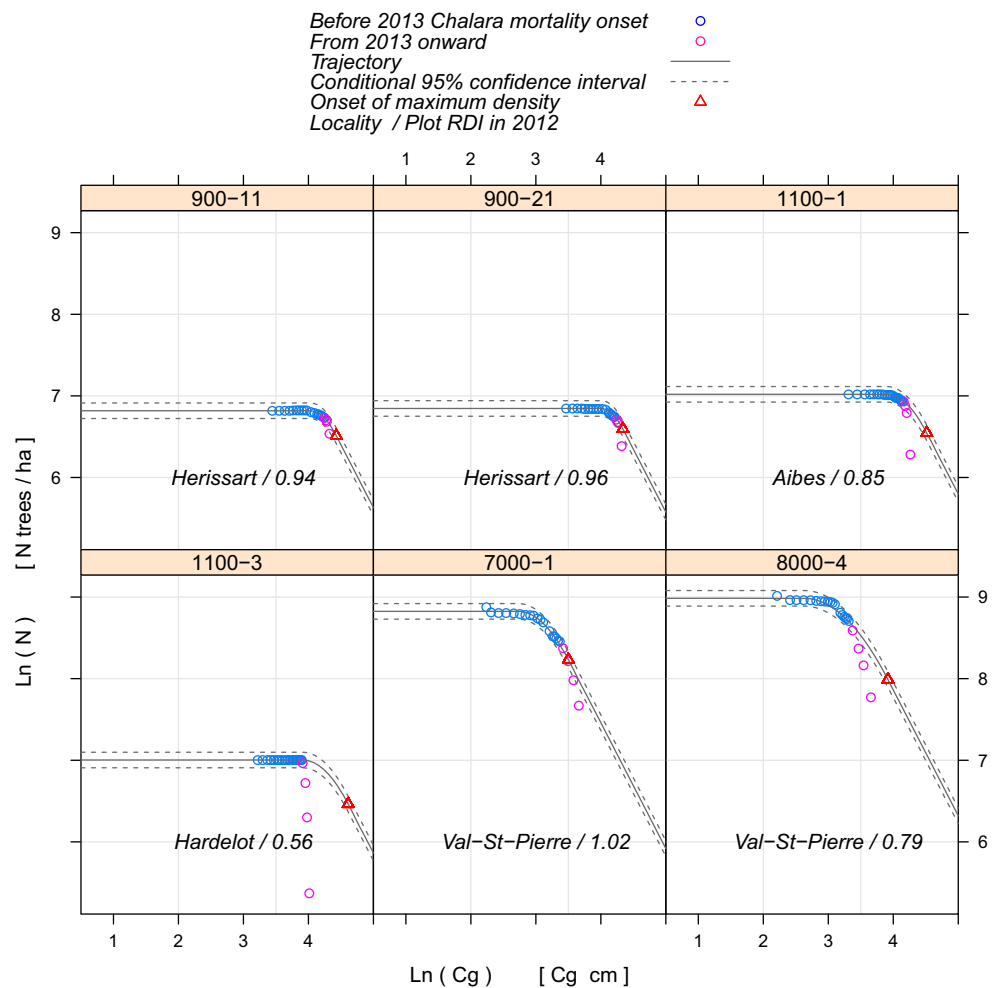
not a complete replacement, and trees will continue to decline. It is estimated that in pure stands of ash only 1 to 2% of trees are totally asymptomatic, 7 years after disease appearance (Husson 2018). For the permanent sample of trees of our study, the cumulated mortality due to ash dieback, from the first signs of dieback (2012) until 2018, amounts from 20 to 80% depending on plot (Fig. 5). It is then unlikely that stands could regain a size-density trajectory similar to that of an unaffected stand[10] or even of a thinned stand of lower initial density, as it could be observed with beech, for example (Ningre et al. 2016a). But data on a longer period and for different stand conditions (initial density, age, fertility) would be necessary to empirically fit size-density trajectories of ash stands subjected to *Chalara* ash dieback.

4.5 Mortality and size class of trees

The monitoring of ash dieback for a sample of trees of different size classes representative of the stand in six of the

experimental plots of our ash network showed that all size classes can be affected, but generally at a larger extent small size classes, more especially in stands at high initial density (Fig. 4). To this extra mortality must be added the self-thinning mortality that affects also preferentially the smaller size classes, which explains partly the departure of the size-density trajectories of ash stands affected by ash dieback from the ones where only competition induced mortality (density-dependent) occurs. In fact, it seems that ash dieback accelerates the mortality process for suppressed trees but works alone for dominant and co-dominant trees.

4.6 Management of stands with *Chalara* ash dieback

Unfortunately, ash is now subject to ash dieback, nearly everywhere in France.

Silvicultural strategies for ash stands in response to ash dieback are presented in Skovsgaard et al. (2017) and Marzano et al. (2019). But for Marçais et al. (2017), the observed levels of mortality in the pole size stands prevent ash stands from any sort of management.

---

[10] Although this was observed by Drew and Flewelling (1977) in the case of *Pinus radiata* plantations impacted by Sirex

Infection by *H. fraxineus*, as insect outbreaks, can be considered as a "fast variable" in the mortality process affecting ash stands (see Neumann et al. 2017). Then, the usual and repeated diameter inventories performed in forest stands could provide a measurable signal of ash dieback in ash stands and judge of its intensity by reporting the size-density trajectories of the stands, compared with the expected ones for the same initial densities, as developed before.

A unique inventory may also be sufficient to detect ash dieback in case the stand density (N) appears well below the expected one for a non-infected stand of same mean girth Cg and initial density. A stand density management diagram (SDMD), with characteristic RDI lines drawn (see Ningre et al. 2019) and size-density trajectories represented for a large range of initial densities, would then allow to see quickly, even in the field, if a stand presents an excess mortality and is then probably subject to *H. fraxineus* infection.

Moreover, early warnings of tree dieback and mortality due to *H. fraxineus* infection may be found, for example, on the basis of yearly basal area growth fluctuations in the case where a basal area growth model established for non-infected trees would be available (ongoing study), as infected trees would show less growth than that predicted by the model (by analogy with the work of Camarero et al. 2015).

5 Conclusion

The piecewise model used to represent the size-density trajectories of pure even-aged stands of beech, oak, and Douglas-fir proved its ability to represent the size-density trajectories of a new species, ash, until stands get infected by the *H. fraxineus*. Thus, as for the other species studied, natural mortality appeared to happen at a constant relative density, independently of initial stand density. But this relative density was higher for ash, and then, ash appeared to be more efficient than other hardwoods like oak and beech as it required less growing space for given dimensions, especially in the young stages of stand development.

Ash dieback modified the course of the size-density trajectories of ash stands by an increase of the mortality of trees in comparison with that normally observed in unthinned stands and undergoing density-dependent mortality. This can help to detect tree dieback due to *H. fraxineus* in even-aged ash stands, as it is today the main factor of ash dieback. But more research is necessary to explain the variations of the response of stands,

depending on the age and intensity of infection and on the stand and site conditions.

Thus, size-density trajectories appeared as a baseline to detect tree dieback in unthinned even-aged ash stands and might be well adapted to other species for which such size-density trajectories are available, independently of the origin of tree dieback (biotic or abiotic): this could apply to beech, oak, and Douglas-fir in France (see Ningre et al. 2016a, 2016b, 2019).

Other causes of mortality could occur for ash, for example, non-favorable climatic conditions, but ash dieback symptoms are clear (crown decline and also collar girdling, Marçais et al. 2017) and get worse over time, which explains the high level of mortality often observed after only a few years of infestation and the departure from expected size-density trajectory.

Compliance with ethical standards

Annex

Fig. 9 Picture of Chalara ash dieback in an ash experimental stand of the east of France showing trees with different levels of defoliation

Fig. 8 Pictures of a sample of the experimental plots of ash retained to modelize the size-density trajectories of even-aged stands of ash: Aibes (2005), Val-St-Pierre (2005), Arracourt (2006) (from left to right and top to bottom). Image source : Canta, René. INRA Nancy

INRA≥ Springer

Fig. 10 Details on the fitting process of size-density trajectories of ash: commented functions of the R environment for statistical computing and its *nlme* package used to fit the mixed model to the ash data discussed in the study (R Development Core Team 2012)

```
Commented R code

## Equation (1): x0, y0, and x stand for Ln(Cg0), Ln(N0), and Ln(Cg).
## a and b stand for a and b in the text.
full.param.traj <- function(a, b, x0, y0, x) {
    x1 <- (2 * (y0 - a) - b * x0) / b
    ## x1 stands for Ln(Cg1) in the text, where Cg1 is the mean
    ## girth for which the stand reaches maximum size-density.
    s <- (b * b) / (y0 - a - b * x0)
    p <- y0 + s * (x0 * x0) / 4
    q <- -s * x0 / 2
    r <- s / 4
    y <- ifelse(x < x0, y0,
            ifelse(x < x1, p + q * x + r * x * x,
               a + b * x))
    return(y)
}

## Equation (1) with constraint between Ln(N0) and Ln(Cg0).
## a, b, and a1 stand for a, b, and a1 in the text.
constrained.param.traj <- function(a, b, a1, y0, x) {
    x0 <- (y0 - a1) / b ## The constraint.
    return(full.param.traj(a, b, x0, y0, x))
}

## The fitting function of R nlme package.
nlme.fit <- nlme(model = y ~
    constrained.param.traj(a, b, a1, log(n0), x),
    ## a, b, a1, and n0 are the parameters to estimate.
    ## They stand for a, b, a1, and N0 in the text.
    ## x is the independent variable Ln(Cg),
    ## y is Ln(N).
    data = ash.data, method = "ML",

    ## Fixed parameters ...
    fixed = list(a ~ 1, b ~ 1, a1 ~ 1, ## common to all treatments, ...
      n0 ~ -1 + grp), ## and treatment dependant.
    random = list(stand = a ~ 1), ## Random effect on a.
    start = list(fixed = c(a = a.strt, b = b.strt, a1 = a1.strt, n0 = n0.strt)),

    correlation = corARMA(form = ~ year | stand, p = 1, q = 1),
    ## Autoregressive moving average autocorrelation between error
    ## terms (within stands), with respective p and q parameters.

    weights = varIdent(form = ~ 1 | w.grp) ## Heteroscedasticity of error terms.
    )
```

Parameters of the size-density model to be estimated

The only parameters of interest to define Eq. (1) and for the fitting process are the parameters a, b, N_0, and Cg_0. The values Cg_1 and RDI_0 are not needed to define Eq. (1) and are totally unknown to the fitting process (Annex, Fig. 10). Everywhere they can be replaced by their expressions as functions of the parameters a, b, N_0, and Cg_0, and such are the values p, q, and r. The only reasons why these values appear in the text are that (a) they help to condense the definition of Eq. (1), and (b) these values have a particular meaning, which is self-evident for RDI_0, Cg_1 being the stand girth at the onset of maximum density (see Fig. 1 in Ningre et al. 2019).

Fitting process

The *R* function, in *R* parlance, *nlme* has a syntax—and corresponding functionality—that allows to fit altogether to a data set parameters that are common to groups (our data, in that particular instance, are grouped by "treatments" or groups of comparable initial density) and parameters that change from one group to the other (see Annex, Fig. 10).

The constraint on the parameters N_0 and Cg_0 was expressed by an algebraic equation (see & 2.3 of the article and Annex, Fig. 10), which moreover was algebraically solvable. Consequently, in the fitting process, this constraint could be accounted for straightforwardly, substituting N_0 for Cg_0, with the parameters a_1 and b.

Fig. 11 The autocorrelation plot of the normalized within group residuals showed that all one-year lag autocorrelations were located within the 99% confidence interval on 0, corresponding to no significant evidence of autocorrelation between these residuals
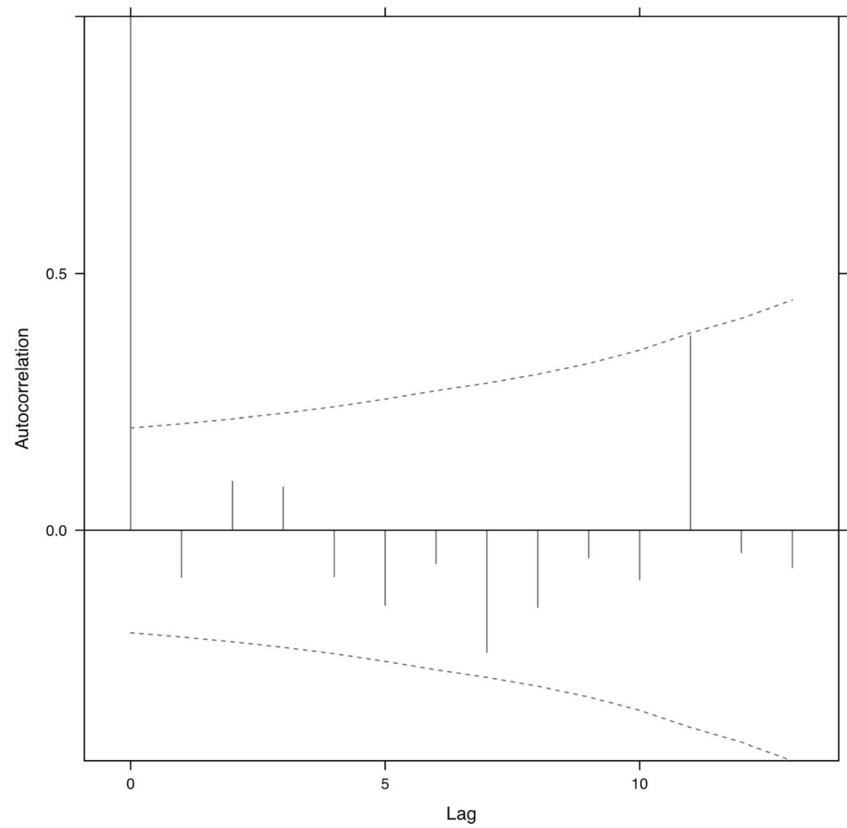
Fig. 12 Normal (QQ) plot of the normalized residuals of the fit of Eq. (1) to the ash stand data with the linear constraints on the inflection points. The linearity of the relationships suggested there was no evidence for a significant departure from normality of the withingroup (treatment) errors
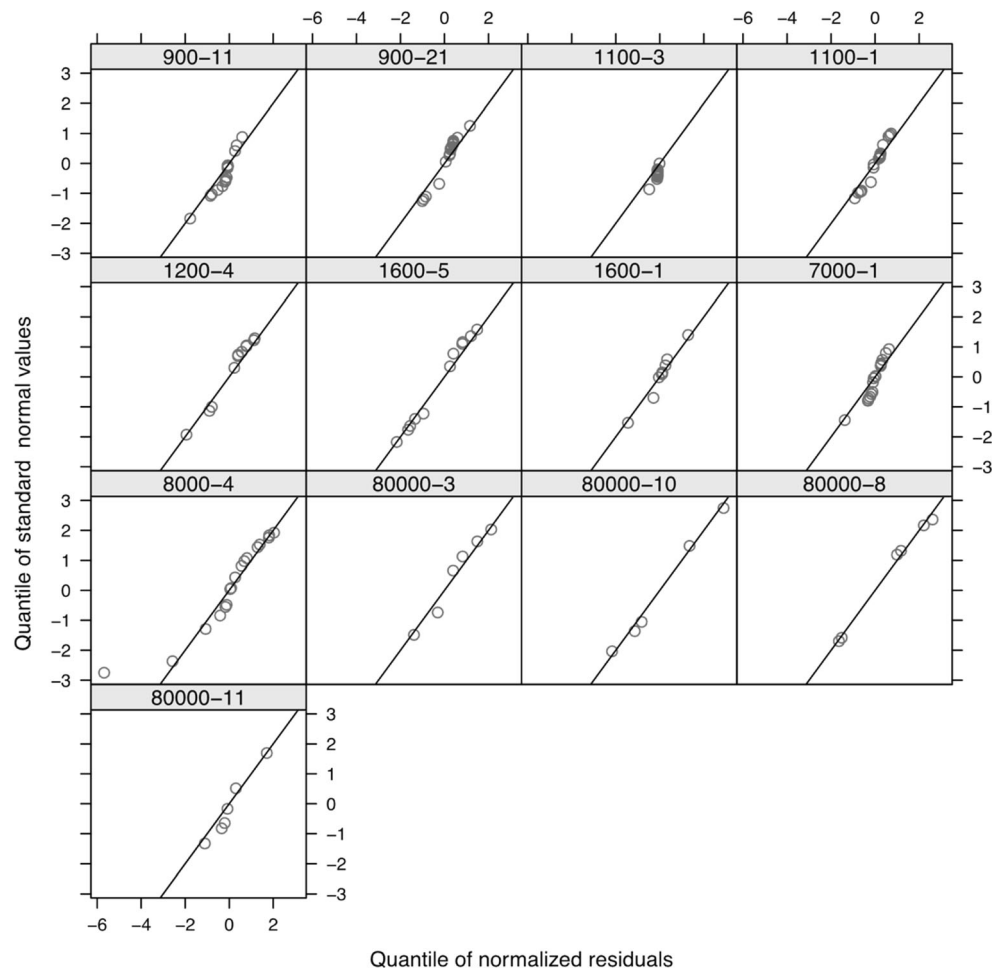
Fig. 13 Normal (QQ) plot assessing the normality of the random effect for the parameter *a*
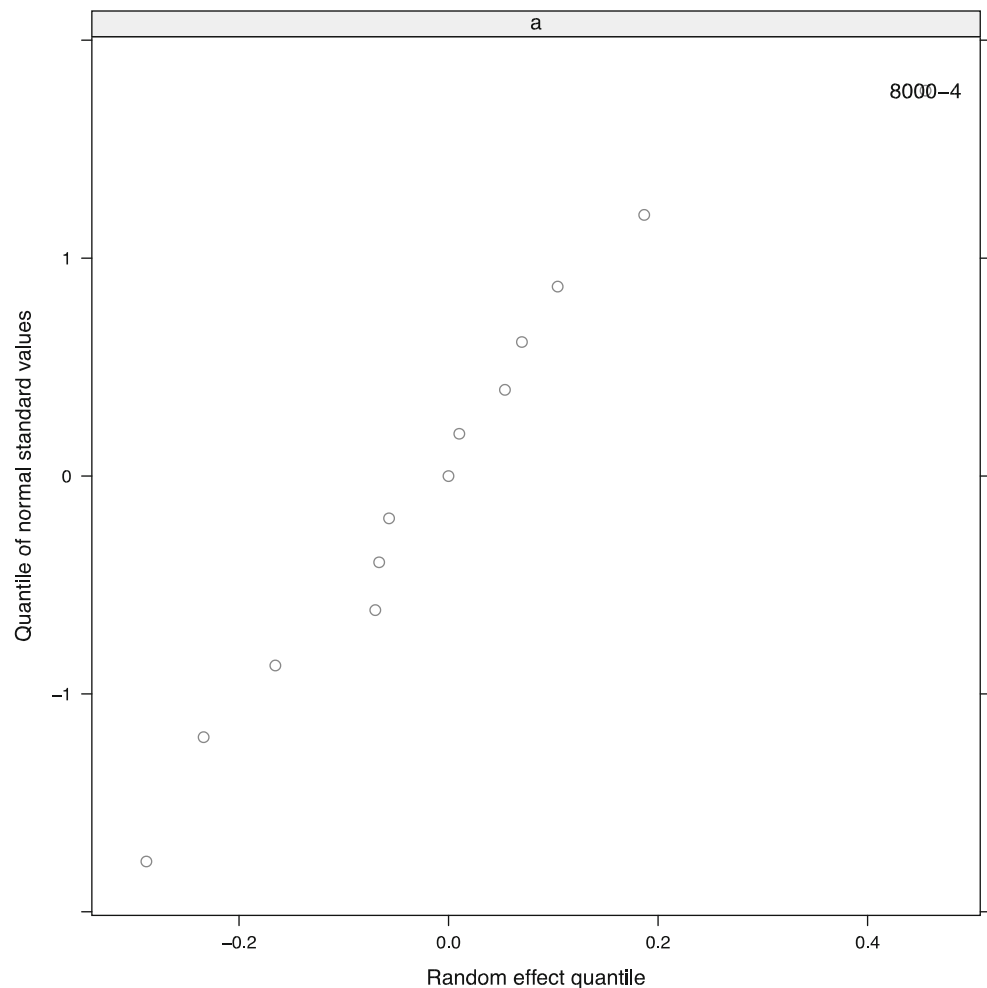
References

Camarero JJ, Gazol A, Sangüesa-Barreda G, Oliva J, Vicente-Serrano M (2015) To die or not to die: early warnings of tree dieback in response to a severe drought. J Ecol 103:44–57

Drew TJ, Flewelling JW (1977) Somme recent japanese theories of yield density relationships and their application to Monterey pine plantations. For Sci 23:517–534

Ge F, Zeng W, Ma W, Meng J (2017) Does the slope of the self-thinning line remain a constant value across different site qualities? –An implication for plantation density management. Forests 8(10):355. https://doi.org/10.3390/f8100355

Goudet, M., Piou, D. (2012) *Chalara fraxinea* sur frêne, situation fin 2012 Bilan de la santé des forêts 2012, Département de la santé des forêts, Ministère de l'Agriculture de l'agroalimentaire et de la forêt, France, Dec 2012

Goudet, M., Saintonge, F.-X., Nageleisen, L.-M. (2018) Quantifier l'état de santé de la forêt, méthode simplifiée d'évaluation. Source et documents techniques: Note de service DGAL/SDQSP/2018-433, Département de la Santé des Forêts, Ministère de l'Agriculture et de l'Alimentation, Paris, France

Grandjean, P., Macaire, A. (2009) L'émergence d'un nouveau pathogène sur le frêne commun en France: *Chalara fraxinea*, R D V T n°25, pp 3-5

Husson C (2018) L'émergence de la chalarose en France. Rev For Fr 70(6):613–620. https://doi.org/10.4267/2042/70311

Johnson PS, Shifley R, Rogers R (2009) The ecology and silviculture of oaks, 2nd edn. CAB international, Wallingford, p 580

Le Goff N, Ottorini J-M, Ningre F (2011) Evaluation and comparison of size-density relationships for pure even-aged stands of ash (*Fraxinus excelsior L.*), beech (*Fagus silvatica L.*), oak (*Quercus petraea Liebl.*), and sycamore maple (*Acer pseudoplatanus L.*). Ann For Sci 68:461–475. https://doi.org/10.1007/s13595-011-0052-8

Lhotka JM, Loewenstein EF (2008) An examination of species-specific growing space utilization. Can J For Res 38:470–479. https://doi.org/10.1139/X07-147

Long JN, Vacchiano G (2014) A comprehensive framework of forest stand property– density relationships: perspectives for plant population ecology and forest management. Ann For Sci 71:325–335. https://doi.org/10.1007/s13595-013-0351-3

Long JN, Dean T, Roberts SD (2004) Linkages between silviculture and ecology: examination of several important conceptual models. For Ecol Manag 200:249–261. https://doi.org/10.1016/j.foreco.2004.07.005

Manion PD, Griffin DH (2001) Large landscape scale analysis of tree death in the Adirondack Park, New York. For Sci 47:542–549

Marçais B, Husson C, Cael O, Dowkiw A, Saintonge F-X, Delahaye L et al (2017) Estimation of ash mortality induced by *Hymenoscyphus fraxineus* in France and Belgium. Balt For 23:159–167

Marzano M, Woodcok P, Quine CP (2019) Dealing with dieback: forest manager attitudes towards developing resistant ash trees in the United Kingdom. Forestry 92:554–567. doi:https://doi.org/10.1093/forestry/cpz022

Neumann M, Mues V, Moreno A, Hasenauer H, Seidl R (2017) Climate variability drives recent tree mortality in Europe. Glob Chang Biol 23(11):4788–4797

Ningre, F. (2020) Dynamics of pure even-aged ash (*Fraxinus excelsior* L.) stands in view to modelizing "size-density" trajectories of unthinned ash stands, with application in evaluating the impact of *Chalara* dieback on ash mortality. [dataset]. V3. Data INRAE repository. https://doi.org/10.15454/OMMABO

Ningre F, Ottorini J-M, Le Goff N (2016a) Modelling size-density trajectories for even-aged beech (*Fagus silvatica* L.) stands in France. Ann For Sci 73:765–776. https://doi.org/10.1007/s13595-016-0567-0

Ningre F, Ottorini J-M, Le Goff N (2016b) Trajectoires d'autoéclaircie du Douglas (*Pseudotsuga menziesii*) en France. Rev For Fr LXVIII(4): 323–343

Ningre F, Ottorini J-M, Le Goff N (2019) Modeling size-density trajectories for even-aged oak (*Quercus petraea Liebl.*) stands and comparison with beech (*Fagus silvatica* L.) in France. Ann For Sci 76:73. https://doi.org/10.1007/s13595-0190855-6

Pilard-Landeau, B., Le Goff, N. (1996) 2 - Sylviculture du Frêne, in: ONF, Bull Tech n°31, Octobre 1996, pp. 9–14

R Development Core Team, Foundation for Statistical Computing (Vienna, Austria). (2012) A language and environment for statistical computing. ISBN 3–900051–07-0. url=http://www.R-project.org/

Reineke LH (1933) Perfecting a stand-density index for even-aged forests. J Agric Res 46:627–638

Skovsgaard JP, Wilhelm GJ, Thomsen IM, Metzler B, Kirisits T, Havrdova L, Enderle R, Dobrowolska D, Cleary M, Clark J (2017) Silvicultural strategies for *Fraxinus excelsior* in response to dieback caused by *Hymenoscyphus fraxineus*. Forestry 90:455–472

Van Miegroet, H. (1956) Untersuchungen über den Einfluss der waldbaulichen Behandlung und der Umweltsfaktoren auf den Aufbau und die morphologischen Eigenschaften von Eschendickungen im schweizerischen Mittelland. — Annales de l'Institut fédéral suisse de Recherches forestières, vol. 32, n° 1, 1956, pp. 229–370